International Journal of GEOMATE, Sep., 2024 Vol.27, Issue 121, pp.33-40
ISSN: 2186-2982 (P), 2186-2990 (O), Japan, DOI: https://doi.org/10.21660/2024.121.4443
Geotechnique, Construction Materials and Environment

COMPARING THE DYNAMIC RESPONSE OF A LAYERED GROUND TO DIFFERENT TRAINLOADS

*Pham Ngoc Thach

Institute of Civil Engineering, Hochiminh City University of Transport, Vietnam

*Corresponding Author, Received: 09 Feb. 2024, Revised: 16 July 2024, Accepted: 17 July 2024

ABSTRACT: The problem of ground dynamic response to a high-speed trainload has received much research attention in the literature, ranging from simplified analytical studies for elastic half-space to sophisticated numerical studies for layered or improved grounds. While most studies have focused on the dynamic response of a ground to a particular trainload, limited attention has been paid to comparing the dynamic response of a ground to different trainloads. In this study, we simulate the dynamic response of a layered ground to the passage of X2000 and Shinkansen trainloads. The obtained results are then compared to gain an understanding of how the ground responds to different trainloads. It is found that because the X2000 train and the Shinkansen train differ in carriage weights, carriage lengths, bogie distances and axle distances, they produce two trainloads whose magnitude and distribution of axle loads are different. As a consequence, they result in a difference in the surface deflection and displacement amplitudes. The difference in displacement amplitudes between the two train cases happens not only at the critical speed but also at all other considered train speeds (from 72 km/h to 360 km/h). On the other hand, although the X2000 train and Shinkansen train produce 2 trainloads that are different in magnitude and distribution of axle loads, they still result in the same critical speed of 252 km/h. This implies that the critical speed does not depend on the trainload type. Instead, it depends mainly on the specific wave propagation characteristics of the ground.

Keywords: Ground vibration, High-speed train, Critical speed, Finite element method

1. INTRODUCTION

For long-distance travel, the comfort and energy efficiency associated with railway transport have made this transport system very competitive when compared with air and road transport. Therefore, in recent decades, more and more high-speed railway lines have been constructed in many countries around the world [1-4]. Besides the advantages of railway transport, there are also adverse problems arising from high-speed railway traffic. Among them is the problem of train-induced ground vibration.

Trains generate ground vibration when they run at high speeds. The intensity of ground vibration generally becomes larger as the train speed increases. Especially when the train speed is comparable to some natural wave speeds of the ground, the ground vibration is particularly high [5,6]. For a given trainload and ground condition, a train speed at which the trainload causes maximum ground response is called a critical speed. Both theory findings and field observations have shown that the intensive ground vibration induced when trains run at high speeds really raises a safety concern for high-speed trains [6-8]. Therefore, the analysis of ground vibration caused by the passage of a high-speed train has received much research attention in the literature, ranging from simplified analytical investigation for elastic half-space [9,10] to sophisticated numerical investigation for layered grounds [6,11,12] and improved grounds [13-15].

While most of the cited studies have focused on the dynamic response of a given ground to a particular trainload, limited attention has been paid to comparing the dynamic response of a ground to different trainloads. Specifically, for a given area with a specific ground condition, there may be some train types running through this area. Each train type has specific carriage weights, carriage lengths, bogie distances and axle distances. Therefore, different train types produce trainloads whose magnitude and distribution of axle loads are different. These trainloads thus contain different frequency excitation content and may excite different modal modes of ground vibration. This implies that the trainload type may have a significant influence on the characteristics of ground vibration.

In this study, we simulate the dynamic response of a layered ground to the passage of X2000 and Shinkansen high-speed trains. The obtained results are then compared and discussed to gain an understanding of how the ground responds to different trainloads.

2. RESEARCH SIGNIFICANCE

The preceding literature review indicates that while most studies have focused on the dynamic response of a given ground to a particular trainload, limited research attention has been paid to the dynamic response of a ground to different trainloads. Therefore, we compare the dynamic response of a

layered ground to the passage of X2000 and Shinkansen trains. Because these trains differ in carriage weights, carriage lengths, bogie distances and axle distances, they represent 2 trainloads whose magnitude and distribution of axle loads are different. The significance of this study is therefore to provide an understanding of how the trainload type affects the characteristics of ground vibration, in particular the critical speed, surface deflection and vibration amplitudes.

3. TRAINLOADS, GROUND PROFILE AND FINITE ELEMENT MODEL

3.1 Trainloads

Two train types selected in this study are X2000 and Shinkansen, which have been commonly used in previous studies [6,11,12,16]. Their trainloads are shown in Fig. 1 and Fig. 2. For high-speed railways, the contact surface between rails and wheels is of very high quality; this study therefore assumes that the contact between rail and wheel is perfect and that the axle loads act on the rails as constant-magnitude moving loads. Besides, a train can have many carriages. However, in this study, the number of carriages is assumed to be 5 carriages. According to Thach [16], this number of carriages should be enough to represent a full-length train with many carriages; if more train carriages are used, we still get the same result, but the computational cost may increase significantly. When comparing the two trains, it can be observed that they have different carriage weights, carriage lengths, bogie distances and axle distances. Therefore, they represent two trainloads whose magnitude and distribution of axle loads are different.

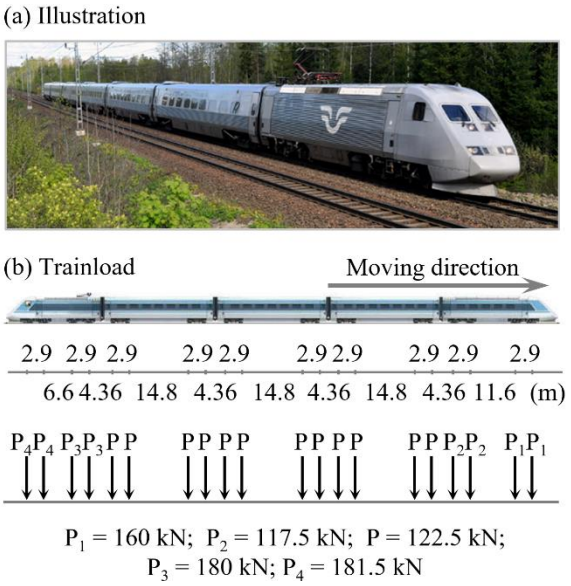

Fig. 1 X2000 train

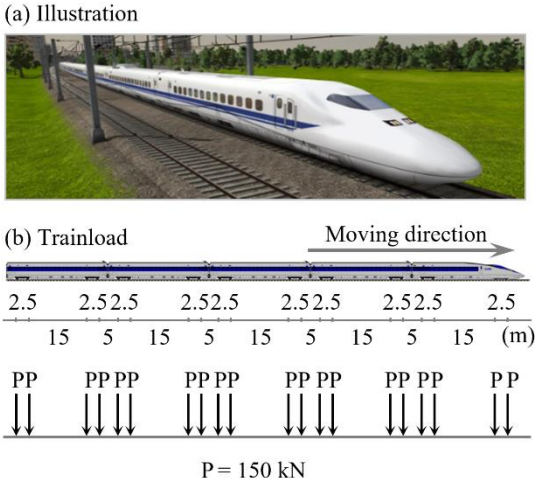

Fig. 2 Shinkansen train

3.2 Ground Profile

The ground profile in reference [6] is assumed in this study. It is a layered ground as shown in Fig. 3, which includes ballast, sand 1, clay 1, clay 2 and sand 2 overlaying on the bedrock. Material parameters are given in Table 1; in which, ρ, VS and VR are mass density, characteristic shear wave speed and Rayleigh wave speed, respectively.

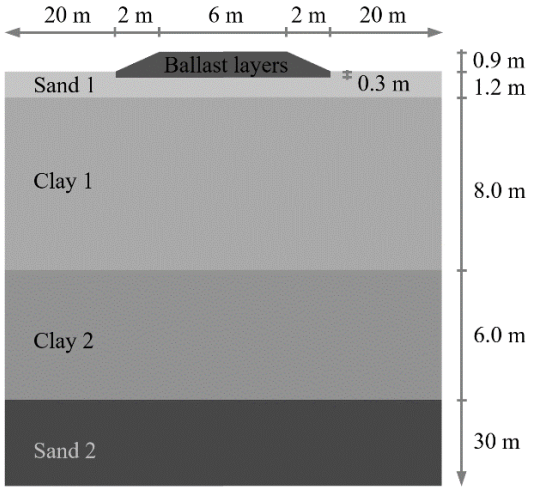

Fig. 3 Ground profile

Table 1. Material parameters

Material	ρ (kg/m^3)	V_S (m/s)	V_R (m/s)
Ballast	2000	210	194.8
Sand 1	1900	63	58.5
Clay 1	1800	60	55.7
Clay 2	1800	87	80.7
Sand 2	1850	98	90.9

3.3 Finite Element Model

Fig. 4 shows the finite element model, which is built with the aid of the program ABAQUS [17]. The complex geometry of ballast and soil layers is meshed by C3D8R elements, which are 8-node hexahedral finite elements with reduced integration and hourglass control [17,18]. At the bottom of the model, a fixed boundary condition is used to represent the bedrock. On 4 sides of the model, if a fixed boundary condition is used, waves generated by a trainload will be reflected on the boundary and consequently result in a meaningless response at observation points of interest. To minimize the influence of wave reflection, we create an absorbing boundary condition on the model sides by using CIN3D8 elements, which are infinite elements that are capable of absorbing elastic waves hitting normal to the element face [17,19]. The model has a total of 4592700 finite elements and 93312 infinite elements.

Because soils are multi-phase materials that generally consist of solid, liquid and air phases, the real behavior of soils under dynamic loading is very complex. As a consequence, many studies on train-induced ground vibrations have simplified the complexity by modeling soils as single-phase materials [9-16]. Based on this simplification, this study assumes that the materials are single-phase and behave elastically with three material parameters: mass density, shear wave speed and Rayleigh wave speed [20]; whose values are given in Table 1. Rayleigh damping is used to represent all mechanisms of energy dissipation [17,21], in which the mass and stiffness proportional damping constants are selected to provide damping ratios of 3% to 6% in the frequency range of 3 Hz to 40 Hz. A lumped mass model is used to represent the continuous distribution of mass within each finite element [17,21]. The finite element equations of motion are integrated numerically by the explicit half-step central difference method [17-19].

For a trainload with a particular moving speed, the ground response to the trainload is simulated in two major steps. First, the trainload is transferred to the ballast surface as a series of equivalent concentrated forces by using the method presented in [19]. Then, we use the finite element model presented above to simulate the ground response to the equivalent forces.

To verify the finite element modeling approach, we consider the problem: a unit axle load moving on a track resting on an elastic half-space. The moving speed is 216 km/h. The density, Rayleigh and shear wave speed of the half-space are 1800 kg/m3, 60.3 m/s, and 65 m/s, respectively. The problem is solved by the finite element method and an analytical method. The finite element model of the considered problem is shown in Fig. 5. The analytical method was developed by [9], which provides a frequency-domain analytical solution to train-induced ground vibration velocity for the case of a track resting on an elastic half-space. Fig. 6 shows the Fourier amplitude spectrum of vertical velocity at the observation point resulting from both methods. It can be observed from the figure that the finite element solution represents the velocity amplitude at all important frequencies well.

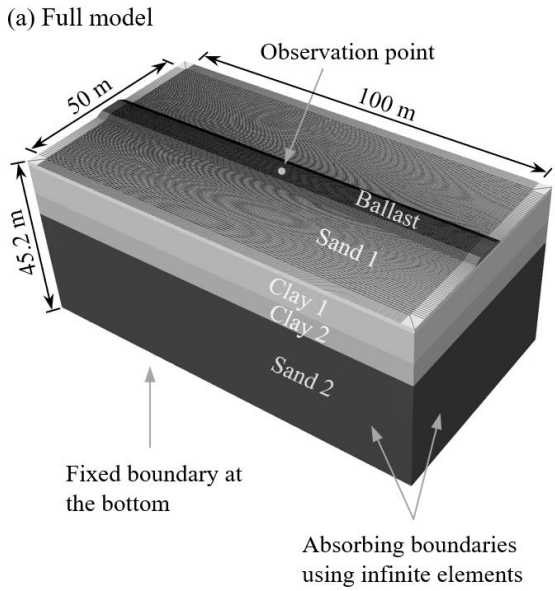

Fig. 4 Finite element model

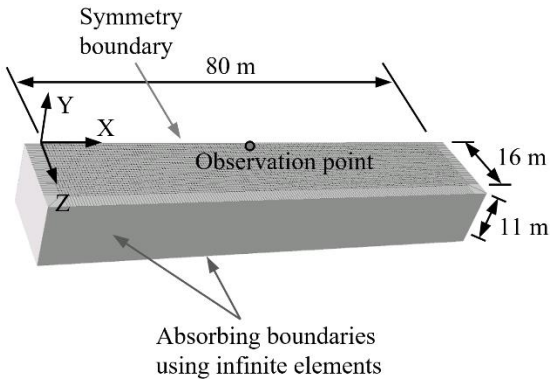

Fig. 5 FEM model of the verification problem

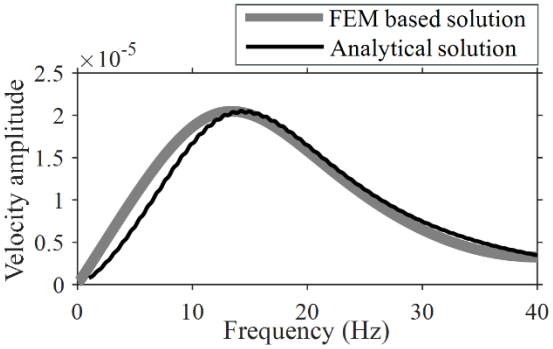

Fig. 6 Amplitude spectrum of vertical velocity

4. RESULTS AND DISCUSSION

4.1 Critical Speed

Let's focus on the observation point marked in Fig. 4, which represents a location on the ballast surface. When each train passes this point, its vertical displacement time history is recorded and presented in Fig. 7 (X2000) and Fig. 8 (Shinkansen) for 9 cases of train speed ranging from 72 km/h to 360 km/h. For each time history in Fig. 7 and Fig. 8, the largest positive and negative displacement values are selected. These values are summarized in Fig. 9 as displacement amplitude versus train speed.

It can be observed from Fig. 9 that, for the X2000 train, the ground surface displacement is maximally amplified at a speed of 252 km/h. This observation indicates that the critical speed is 252 km/h. At this critical speed, the negative and positive displacement amplitude are 6.4 mm and 0.8 mm, respectively. Fig. 9 also indicates that, for the Shinkansen train, the critical speed is 252 km/h and at this critical speed, the negative and positive displacement amplitude are 5.8 mm and 1.6 mm, respectively. Thus, both trains result in a critical speed of 252 km/h.

The above observations imply that although X2000 and Shinkansen produce 2 trainloads whose magnitude and distribution of axle loads are different, they still result in the same critical speed. In other words, the critical speed does not depend on the trainload type, instead, it depends mainly on the specific wave propagation characteristics of the ground.

4.2 Surface Deflection and Vibration Amplitudes

The time histories in Fig. 7 and Fig. 8 are converted to spatial coordinates through the relationship $d = -vt$, where d is the distance along the rail track, v is the train speed and t is the time. The conversion results are presented in Fig 10 for the X2000 train and Fig. 11 for the Shinkansen train. It should be noted that each graph in Fig. 10 and Fig. 11 is just a ground surface deflection beneath the trainload, which moves with the train.

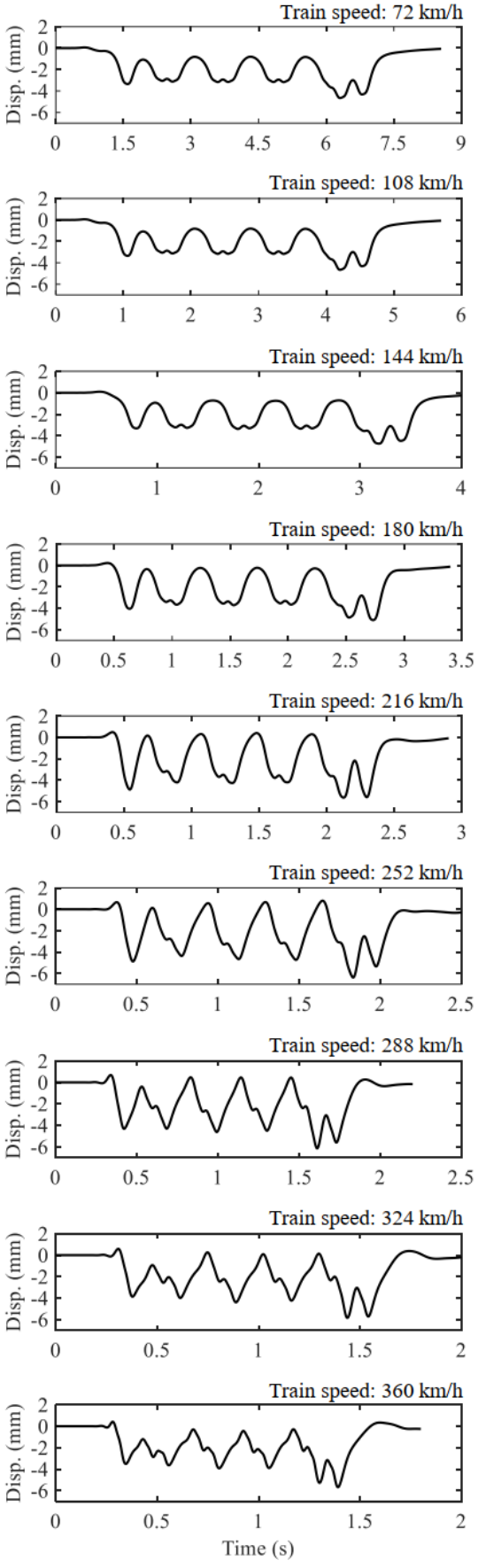

Fig. 7 Displacement time history (X2000)

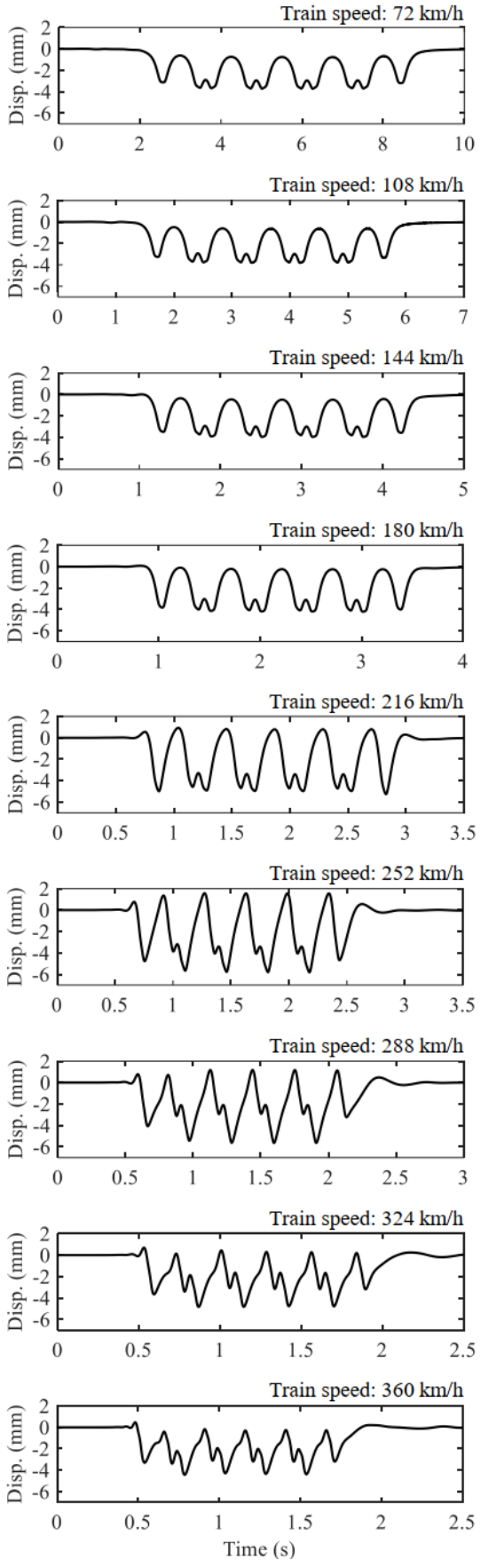

Fig. 8 Displacement time history (Shinkansen)

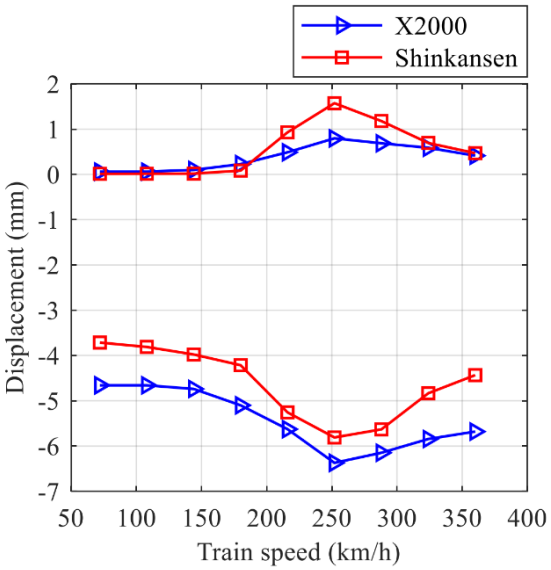

Fig. 9 Displacement amplitude versus train speed

It can be observed either from Fig. 10 or Fig. 11 that the surface deflection for the cases of train speed 72, 108, 144 and 180 km/h is similar in shape and almost only has negative displacement. This observation indicates that when the train speed is low, the ground behaves quasi-statically, namely the displacement field is similar to a static displacement field caused by the train that is at rest. The quasi-static displacement field is illustrated in Fig. 12 for the Shinkansen train. For the cases of train speed greater than 180 km/h, the surface deflection is not similar in shape and has both negative and positive displacements. This observation indicates that when the train speed is high, the ground behaves dynamically and the trainload generates waves propagating on the ground surface as illustrated in Fig. 13 for the Shinkansen train.

The surface deflection at the critical speed of 252 km/h from 2 train cases is compared in Fig. 14. From this figure, the following can be observed. For the X2000 case, the peak displacement in the last carriage is significantly higher than that in the remaining carriages. For the Shinkansen case, the peak displacements in all carriages are nearly equal. The X2000 case gives a larger maximum displacement than the Shinkansen case.

These observations can be interpreted as follows. For the X2000 case, because the weight of the last carriage is significantly larger and the bogie distance is shorter than that of the remaining carriages, the magnitude and distribution pattern of the axle loads in the last carriage differ from the remaining carriages, thus making the displacement peak in the last carriage the largest. For the Shinkansen case, because the carriages have similar weights and bogie distances, the displacement peaks among the carriages are quite equal in magnitude.

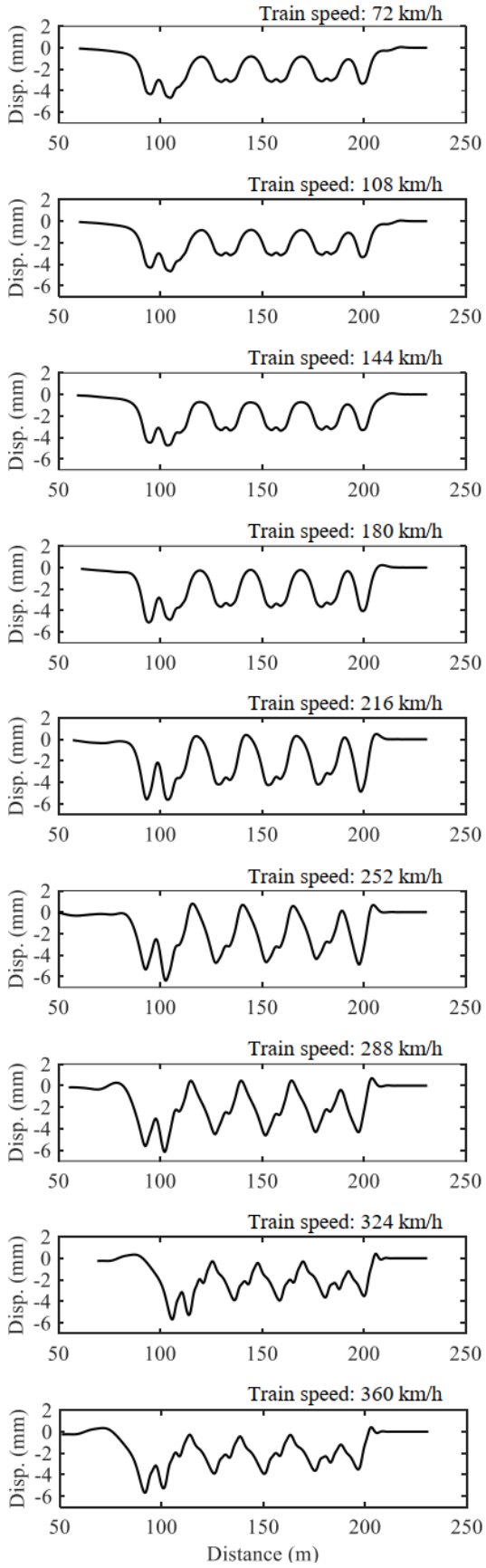

Fig. 10 Surface deflection (X2000)

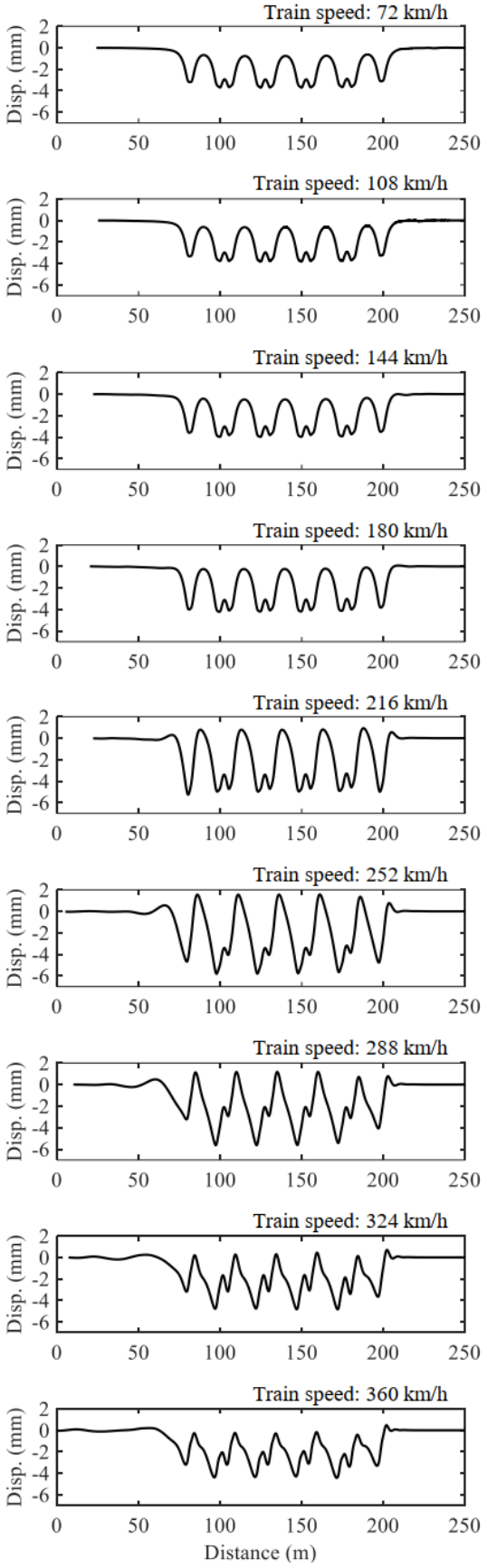

Fig. 11 Surface deflection (Shinkansen)

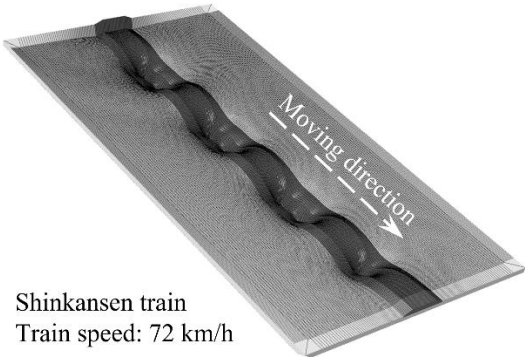

Fig. 12 Displacement field at a low train speed

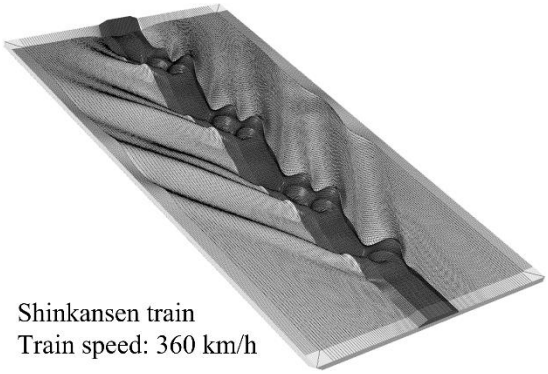

Fig. 13 Displacement field at a high train speed

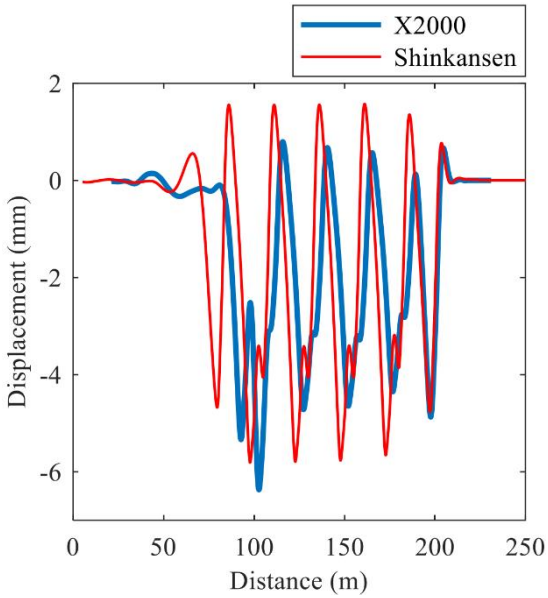

Fig. 14 Comparing surface deflection at 252 km/h

Besides, because the last carriage of the X2000 train weights 723 kN while each carriage of the Shinkansen train weights 600 kN only, the X2000 train results in a larger maximum displacement than the Shinkansen train (6.4 mm vs. 5.8 mm). The difference in displacement amplitudes between the two train cases happens not only at the critical speed but also at all other train speeds as can be observed clearly in Fig. 9.

The above observations indicate that the surface deflection and vibration amplitudes are influenced by the trainload type. More specifically, the X2000 and Shinkansen differ in carriage weights, carriage lengths, bogie distances and axle distances, so they produce two trainloads whose magnitude and distribution of axle loads are different. As a consequence, they result in a significant difference in the surface deflection and vibration amplitudes.

5. CONCLUSION

Trainload type has a significant influence on the train-induced surface deflection and ground vibration amplitudes. Because the X2000 train and the Shinkansen train differ in carriage weights, carriage lengths, bogie distances and axle distances, they produce two trainloads whose magnitude and distribution of axle loads are different. As a consequence, they result in a difference in the surface deflection and displacement amplitudes. The difference in displacement amplitudes between the two train cases happens not only at the critical speed but also at all other considered train speeds (from 72 km/h to 360 km/h).

Although the X2000 train and Shinkansen train produce 2 trainloads that are different in magnitude and distribution of axle loads, they still result in the same critical speed of 252 km/h. This implies that the critical speed does not depend on the trainload type, instead, it depends mainly on the specific wave propagation characteristics of the ground.

6. REFERENCES

[1] Gholamizadeh K., Zarei E. and Yazdi M., Railway transport and its role in the supply chains: overview, concerns, and future direction, in The Palgrave handbook of supply chain management, Sarkis J., Palgrave Macmillan, London, UK, 2022, pp. 1-28.

[2] Purba A., The challenge of developing high-speed rail projects: recent evidence from developing countries, International Journal of GEOMATE, Vol. 18, Issue 70, 2020, pp. 99-105.

[3] Correia A. and Ramos A., A geomechanics classification for the rating of railroad subgrade performance, Railway engineering science, Vol. 30, 2022, pp. 323–359.

[4] Pholkainuwatra P., Eua-apiwatch S. and Yimsiri S., Selection of railway ballast based on cementing potential: a case study in Thailand, International Journal of GEOMATE, Vol. 25, Issue 107, 2023, pp.183-190.

[5] Krylov V., Ground Vibrations from High-Speed Railways: Prediction and Mitigation, 2019, ICE Publishing, London, UK, pp. 1-367.

[6] Thach P., Influence of Train Speed on Ground Vibrations Due to High-Speed Train, Transport and Communications Science Journal, Vol. 75, Issue 5, 2024, pp. 1775-1788.
[7] Ramos A., Pinto C., Colaco A., Ruiz F. and Costa A., Predicting Critical Speed of Railway Tracks Using Artificial Intelligence Algorithm, Vibration, Vol. 6, Issue 4, 2023, pp. 895-916.
[8] He C., Li H., Gong Q. Zhou S. and Ren J., Modelling of critical speed of railway tracks on a multi-layered transversely isotropic saturated ground, Applied Mathematical Modelling, Vol. 121, 2023, pp. 75-95.
[9] Krylov V., Chapter 9: Generation of ground vibration boom by high-speed trains, in Noise and vibration from high-speed trains, Krylov V., Thomas Telford, London, UK, 2001, pp. 251-284.
[10] Yang Y. and Hung H., Wave propagation for train-induced vibrations, 2009, World Scientific, Danvers, Massachusetts, USA, pp. 1-471.
[11] Takemiya H., Simulation of track–ground vibrations due to a high-speed train: the case of X-2000 at Ledsgard, Journal of Sound and Vibration, Vol. 261, Issue 3, 2003, pp. 503-526.
[12] Kacimi A., Woodward P., Laghrouche O. and Medero G., Time domain 3D finite element modeling of train-induced vibration at high speed, Computer and Structures, Vol. 118, 2013, pp. 66-73.
[13] Thach P., Liu H. and Kong G., Evaluation of PCC Pile Method in Mitigating Embankment Vibrations from a High-Speed Train, Journal of Geotechnical and Geoenvironmental Engineering, Vol. 139, No. 12, 2013, pp. 2225-2228.
[14] Thach P., Liu H. and Kong G., Vibration analysis of pile-supported embankments under high-speed train passage, Soil Dynamics and Earthquake Engineering, Vol. 55, 2013, pp. 92-99.
[15] Chango I., Assogba O. and Yan M., Estimating Static and Dynamic Stress Distribution in a Railway Embankment Reinforced by Geogrid and Supported by Pile System, Transportation Infrastructure Geotechnology, Vol. 10, 2023, pp. 283-310.
[16] Thach P., Influence of the number of train carriages on train-induced ground vibrations, International Journal of GEOMATE, Vol. 26, Issue 114, 2024, pp. 60-67
[17] Dassault Systèmes, ABAQUS 6.16 theory manuals, 2016, Providence, RI, USA.
[18] Belytschko T., Liu W., Moran B. and Elkhodary K., Nonlinear finite elements for continua and structures, 2014, John Wiley & Sons, New Jersey, USA, pp. 1-804.
[19] Thach P., Chapter 11 Finite-element approach to train-induced vibrations of pile-supported embankments, in Ground Vibrations from High-Speed Railways: Prediction and Mitigation, Krylov V., ICE Publishing, London, UK, 2019, pp. 319-336.
[20] Saran S., Dynamics of Soils and their Engineering Applications, 2021, CRC Press, Boca Raton, USA, pp. 1-576.
[21] Chopra A., Dynamics of structures, 2023, Pearson, Hoboken, NJ, USA, pp. 1-967.